

Video Article

Template Directed Synthesis of Plasmonic Gold Nanotubes with Tunable IR Absorbance

Colin R. Bridges¹, Tyler B. Schon¹, Paul M. DiCarmine¹, Dwight S. Seferos¹

¹Department of Chemistry, University of Toronto

Correspondence to: Dwight S. Seferos at dseferos@chem.utoronto.ca

URL: <http://www.jove.com/video/50420>

DOI: [doi:10.3791/50420](https://doi.org/10.3791/50420)

Keywords: Chemistry, Issue 74, Chemical Engineering, Materials Science, Physics, Nanotechnology, Chemistry and Materials (General), Composite Materials, Inorganic, Organic and Physical Chemistry, Metals and Metallic Materials, Gold, nanotubes, anodic aluminum oxide templates, surface plasmon resonance, sensing, refractive index, template directed synthesis, nano

Date Published: 4/1/2013

Citation: Bridges, C.R., Schon, T.B., DiCarmine, P.M., Seferos, D.S. Template Directed Synthesis of Plasmonic Gold Nanotubes with Tunable IR Absorbance. *J. Vis. Exp.* (74), e50420, doi:10.3791/50420 (2013).

Abstract

A nearly parallel array of pores can be produced by anodizing aluminum foils in acidic environments^{1,2}. Applications of anodic aluminum oxide (AAO) membranes have been under development since the 1990's and have become a common method to template the synthesis of high aspect ratio nanostructures, mostly by electrochemical growth or pore-wetting. Recently, these membranes have become commercially available in a wide range of pore sizes and densities, leading to an extensive library of functional nanostructures being synthesized from AAO membranes. These include composite nanorods, nanowires and nanotubes made of metals, inorganic materials or polymers³⁻¹⁰. Nanoporous membranes have been used to synthesize nanoparticle and nanotube arrays that perform well as refractive index sensors, plasmonic biosensors, or surface enhanced Raman spectroscopy (SERS) substrates¹¹⁻¹⁶, as well as a wide range of other fields such as photo-thermal heating¹⁷, permselective transport^{18,19}, catalysis²⁰, microfluidics²¹, and electrochemical sensing^{22,23}. Here, we report a novel procedure to prepare gold nanotubes in AAO membranes. Hollow nanostructures have potential application in plasmonic and SERS sensing, and we anticipate these gold nanotubes will allow for high sensitivity and strong plasmon signals, arising from decreased material damping¹⁵.

Video Link

The video component of this article can be found at <http://www.jove.com/video/50420/>

Introduction

When their dimensions approach the penetration depth of light (~50 nm; the nanoscale), noble metals, and most importantly gold, exhibit exquisite size, shape and environment dependent optical properties^{24,25}. On this scale, direct illumination causes a coherent oscillation of conduction electrons known as the surface plasmon resonance (SPR). SPR is highly dependent on nanostructure size, shape, and the dielectric properties of the surrounding medium. There is great interest in characterizing SPR properties in new materials, as SPR-based devices are emerging for use in sub-wavelength optics, SERS substrates, and ultra-sensitive optical sensors^{11-16,26-29}. As such, developing computational methods to more accurately predict how size and structure can vary plasmonic response remains a major goal. The use of AAO membranes affords a convenient way to vary the particle diameter or length, and several important studies use this to correlate measured and calculated plasmonic response with varying particle diameter, length, and aspect ratio^{30,31}. Perhaps the most studied and successful use of plasmonic materials is as refractive index based biosensors. For this, resonances in the red to near infrared (NIR) range (~800 - 1,300 nm) are desirable since they are more sensitive to refractive index change, and lie in the "water window" such that they are transmitted through both water and human tissues. Solution-suspendable nanostructures with SPR peaks in this range open intriguing possibilities for *in vivo* plasmonic biosensing.

Porous AAO has been used to prepare polymer nanotubes or nanowires by electrochemical synthesis or template wetting, and proven to be applicable to a wide variety of materials. AAO membranes are now being used to synthesize solution-suspendable high aspect ratio nanorods and nanostructured arrays that function as high performance plasmonic biosensors or SERS substrates. While AAO membranes have mostly been used as templates for synthesizing solid rods, in some cases it may be desirable for the structure to be hollow. Plasmonic and SERS sensing applications, for example, are surface based, and hollow structures with large surface-area-to-volume ratios may lead to stronger signal generation and higher sensitivity^{14,15,32}. With respect to this, gold nanotubes have been synthesized from various methods including galvanic replacement reactions on silver nanorods³³, electroless plating^{34,35}, surface modification of the template pores^{36,37}, sol-gel methods³⁸, and electrodeposition³⁹⁻⁴¹. These syntheses typically leave poorly formed, porous nanotubes or allow for little control over the size and morphology. Syntheses have also been reported wherein a metallic shell is deposited over a polymer core in an AAO membrane^{42,43}. These syntheses leave the gold nanotubes bound to the substrate and rely on template etching to allow for growth of gold around the polymer, thus they cannot be studied in solution. Moreover, template etching has some potential drawbacks. First, non-uniform pore etching along the template wall may lead to a non-uniform gold shell thickness. Second, significant etching (*i.e.* to make very thick wall tubes) may dissolve pore walls completely.

Very recently, Bridges *et al.* reported an etchant free method to synthesize gold nanotubes in AAO membranes that uses a sacrificial poly(3-hexyl)thiophene core and yields solution-suspendable gold nanotubes with extremely high refractive index sensitivity¹⁵. From that and subsequent work, it was discovered that in order to deposit gold shells around the polymer core without chemical etching, the polymer must be tubular such that there is interior space for it to collapse, and the polymer must be hydrophobic such that it will collapse onto itself rather than adhere to the template pore walls¹⁶. When hydrophilic polymers are used, a gold "sheath" partially covering the polymer core is observed, indicating the polymer core adheres to one of the walls of the template during gold deposition⁴⁴. Herein, the detailed protocol for the synthesis of hollow gold nanotubes that allows for control over length and diameter is described (**Figure 1**). These solution-suspendable gold nanotubes are promising materials for a wide range of applications including plasmonic biosensing or SERS substrates.

Protocol

1. Forming the Silver Working Electrode

1. Secure the AAO membrane substrate top side up on a glass plate using a 2-sided adhesive. Note: minimize the membrane area in contact with the adhesive, as it will clog the pores.
2. Install the glass plate into the substrate holder of the metal evaporator, close the chamber, and evacuate to a pressure of below 1.0 μ Torr.
3. Using a resistive source, evaporate silver pellets (>99.99% purity) onto the substrate at a rate of 0.8 Å/sec until a layer thickness of 100 nm is reached, then increase the evaporation rate to 1.5 Å/sec until a final thickness of 250 nm is reached.
4. Release the AAO membranes by wiping the adhesive layer with a cotton swab wetted with dichloromethane to dissolve the adhesive.

2. Electrodepositing Copper and Nickel

1. Steps 2-3 use a custom two-piece open-face Teflon electrochemical cell designed to hold the AAO membranes in contact with a conductive foil that serves as the working electrode (**Figure 2**). The details of the cell design can be found elsewhere⁴⁵. Clean a Teflon cell by rinsing 3 x 10 sec with acetone, ethanol, then 18.2 M Ω deionized water. Allow the cell to dry in the ambient laboratory air.
2. Place the membrane silver-side down onto a piece of smooth aluminum foil in the Teflon electrochemical cell, sealing the working electrode area with a Viton O-ring (**Figure 2**).
3. Add 3.0 ml of copper plating solution (0.95 M CuSO₄(5H₂O), 0.21 M H₂SO₄) to the Teflon cell. Connect a platinum counter electrode, aqueous reference electrode and the aluminum foil working electrode to a potentiostat using a conventional 3 electrode set-up. Apply a potential of -90 mV vs. Ag/AgCl for 15 min.
4. Disconnect and remove the reference and auxiliary electrodes, keeping the two piece cell and AAO membrane intact with the foil, then rinse the cell under running 18.2 M Ω deionized water. Let the cell soak for 30 min in 5 ml 18.2 M Ω deionized water to remove excess copper plating solution from within the pores.
5. Empty the cell, and add 3.0 ml of commercial nickel plating solution (Watt's Nickel Pure from Technic inc.) and connect the counter reference, and working electrodes as described in step 2.3. Apply a potential of -900 mV vs. Ag/AgCl for 20 min.
6. Disconnect and remove the reference and auxiliary electrodes keeping the two-piece cell and AAO membrane and foil intact. Rinse the cell 3 x 10 sec with 18.2 M Ω deionized water, then let it soak for 30 min in 5 ml 18.2 M Ω deionized water to remove excess plating solution from the pores. Allow the cell to thoroughly dry in the ambient laboratory air overnight.

3. Electropolymerizing the Polymer Core

1. Bring the intact Teflon cell assembly into an inert atmosphere glove box equipped with external connections to a potentiostat.
2. Prepare a solution of 30 mM 3-hexylthiophene in 3.0 ml of 46% boron trifluoride in diethyl ether and add it to the Teflon electrochemical cell.
3. Connect the counter and working electrodes to a potentiostat as described in step 2.3. Add a Ag/AgNO₃ acetonitrile reference electrode and connect as described in step 2.3. Apply a potential of +1,500 mV vs. Ag/AgNO₃ for 10 min. Currents on the order of 0.1 mA indicate a successful deposition (**Figure 3**).
4. Disconnect and remove the reference and auxiliary electrodes keeping the two-piece cell and AAO membrane and foil intact and rinse the cell with 5 ml of acetonitrile in the glove box to remove excess boron trifluoride. Remove the cell from the glove box and rinse with a 5 ml aliquot of ethanol, and then allow the cell to soak in fresh ethanol for 20 min. Rinse the cell again with 5 ml milli-Q 18.2 M Ω deionized water and then allow the cell to soak in 18.2 M Ω deionized water for 20 min. Allow it to dry in the ambient laboratory air.

4. Electrodepositing the Gold Shell

1. Add 3.0 ml of commercial gold plating solution (Orotep 24 RTU from Technic Inc.) to the Teflon cell, mix with a pipette for 2 min to allow the gold plating solution infiltrate the pores completely and induce hydrophobic collapse of the polymer core.
2. Connect the working electrode, counter electrode, and aqueous reference electrode to a potentiostat as in step 2.3, and apply -920 mV vs. Ag/AgCl for varying times (5 min to 5 hr). Currents on the order of 0.5 mA indicate a successful deposition (**Figure 3**). The length of the gold nanotube is determined by the deposition time (**Figure 4**).
3. Rinse the cell under a stream of 18.2 M Ω deionized water and allow it to dry.

5. Removing Sacrificial Material and Isolating the Gold Nanotubes

1. Remove the membrane from the Teflon cell assembly, and dissolve the silver, copper and nickel with a few drops of conc. Nitric acid (> 68%) on the silver coated side. Remove the acid and rinse the membranes 3 x 10 sec with 18.2 M Ω deionized water.
2. Etch the polymer core by immersing the membrane overnight in a 3:1 v/v solution of sulfuric acid and 30% hydrogen peroxide (Caution! This solution is a strong oxidizer and should be handled with care).

3. Remove the acid solution and rinse the membrane under a stream of 18.2 mΩ deionized water. Break the membrane into small pieces and place in a 3.0 ml centrifuge vial, and add 2 ml of an aqueous 3.0 M NaOH solution. Agitate the vial in a heated mixer operating at 1,000 rpm and 40 °C for 3 hr or until the membrane is dissolved.
4. Centrifuge the mixture for 10 min at 21,000 x g, remove the supernatant liquid and replace it with 18.2 MΩ deionized water. Repeat this cycle 3 times. The vial now contains gold nanotubes that can be suspended by gentle sonication. Upon sonication and suspension the solution should appear light purple.

6. Optical Characterization of Gold Nanotubes

1. To measure the optical spectra, centrifuge the solution of gold nanotubes for 10 min at 21,000 x g, remove the supernatant liquid and replace it with D₂O. Repeat this process 3 times.
2. Sonicate the mixture for 30 sec until the solution becomes clear, and transfer the solution into a 1 ml quartz cuvette.
3. Obtain the extinction spectra from 200 nm to 2,000 nm in a UV/vis spectrophotometer, operating in dual beam mode using a cuvette with D₂O as the reference cell. Two absorbances should be present, corresponding to the transverse and longitudinal plasmon modes (**Figure 5**).
4. To measure the solid state spectra, proceed to step 5.2. Stop and place the intact membrane on a glass slide.
5. Wet the membrane and glass slide with D₂O to increase transparency.
6. Attach the membrane secured to a glass slide and mount it in a thin film sample holder for a UV/vis spectrophotometer. Operating in dual beam mode, obtain an extinction spectra from 200 nm to 1,300 nm using a glass slide as the reference.

Representative Results

After each step, one can visibly determine whether or not the synthesis is successful by observing the color of the membrane. After copper deposition (step 2.3) the template will appear purple. During nickel deposition (step 2.5) the template will slowly turn black. After the polymer deposition (step 3.3) the template should appear darker purple/black and more glossy (**Figure 2**). Typical chronoamperograms of successful polymer and gold are included (**Figure 3**). During the final etching step (5.2), the template should appear purple and opaque (**Figure 2**) due to the gold nanotubes SPR. After the membrane is dissolved (step 5.4), the gold nanotubes can be visualized using electron microscopy (**Figure 6**). The gold nanotubes can either be imaged from solution by drop casting onto a copper TEM grid, or as an aligned array grown off a gold base by mounting a sample onto an SEM stage prior to template dissolution. The membrane pore size determines the diameter, which varies between 10 and 250 nm according to the manufacturer's specifications. The length of gold nanotubes depends on the deposition time, which can be tuned from 150 nm to several microns. The standard deviation of lengths is expected to be around 15% (**Figure 4**).

Representative optical spectra for 55 nm diameter structures are included (**Figure 5**). The 55 nm diameter structures exhibit two plasmon modes in solution: the transverse mode lying in the visible region (520 nm) and longitudinal mode lying in the near IR region (~1,200 nm). The position of the transverse mode will vary depending on the length of the nanotube. Nanostructures synthesized in 200 nm pore size templates will appear turbid and brown in solution, and scatter heavily across all wavelengths.

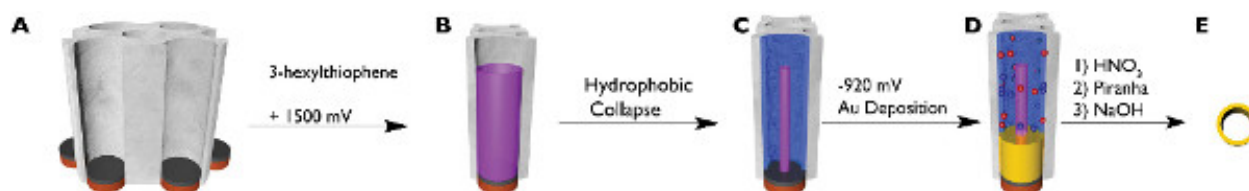


Figure 1. Scheme depicting the procedure for preparing gold nanotubes. One side of the AAO membrane is coated with silver, followed by electrodeposition of the copper and nickel layers within the pores (**A**). The polymer core is deposited (**B**). The polymer core collapses when exposed to water (**C**). The gold shell is deposited (**D**). All sacrificial materials are etched yielding a hollow gold nanotube (**E**). [Click here to view larger figure.](#)

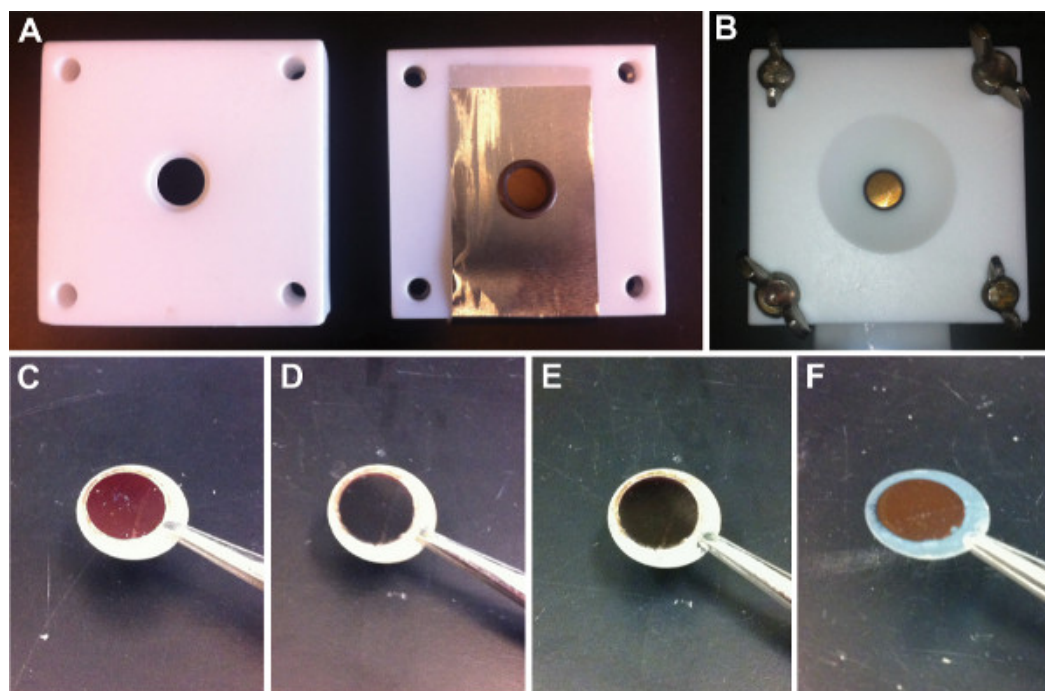


Figure 2. Digital pictures of the Teflon electrochemical cell with a silver coated AAO membrane face down on the aluminum foil before (A) and after (B) assembly. Image of an AAO membrane after copper deposition (C), nickel deposition (D), polymer deposition (E) and gold nanotube deposition after the sacrificial metals and polymer have been etched (F).

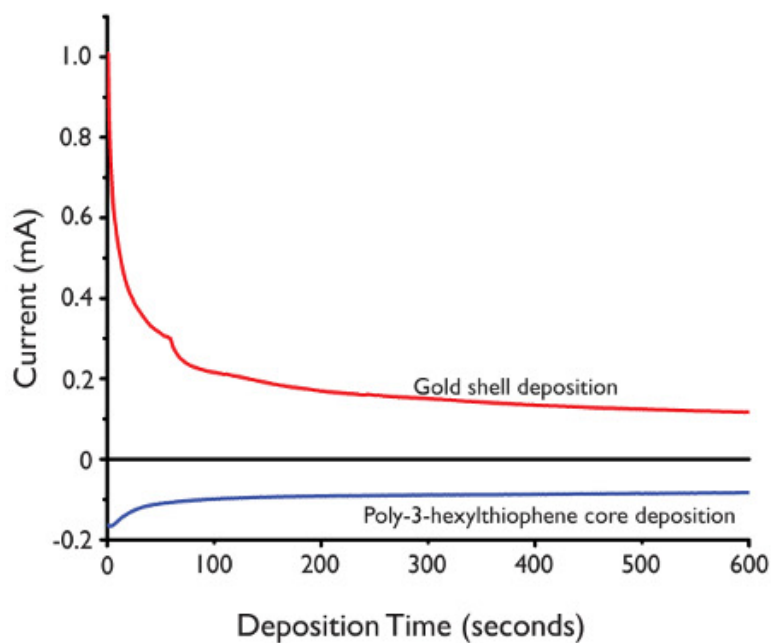


Figure 3. Chronoamperograms of gold nanotube electrodeposition at -920 mV (red) and polymer core electropolymerization at +1,500 mV (blue).

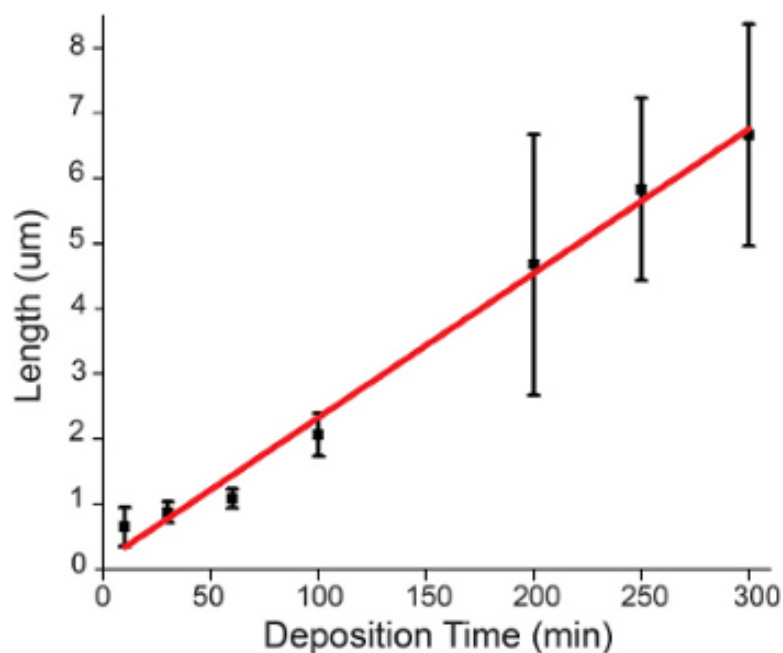


Figure 4. Graph of gold nanotube length versus electrodeposition time at -920 mV for 200 nm gold nanotubes. A linear correlation between length and time is observed. Error bars represent 1 standard deviation in length, based off 100 measurements.

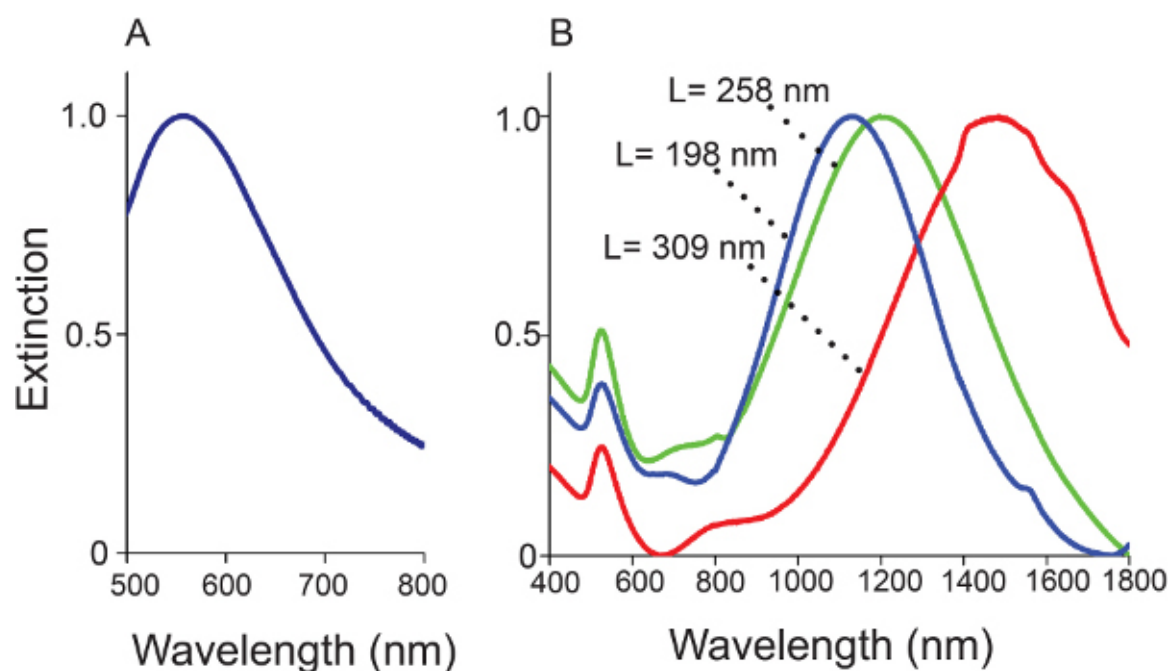


Figure 5. Representative extinction spectra of an aligned array of 55 nm diameter gold nanotubes (A). Representative extinction spectra of solution suspended gold nanotubes as length (L) increases (B).

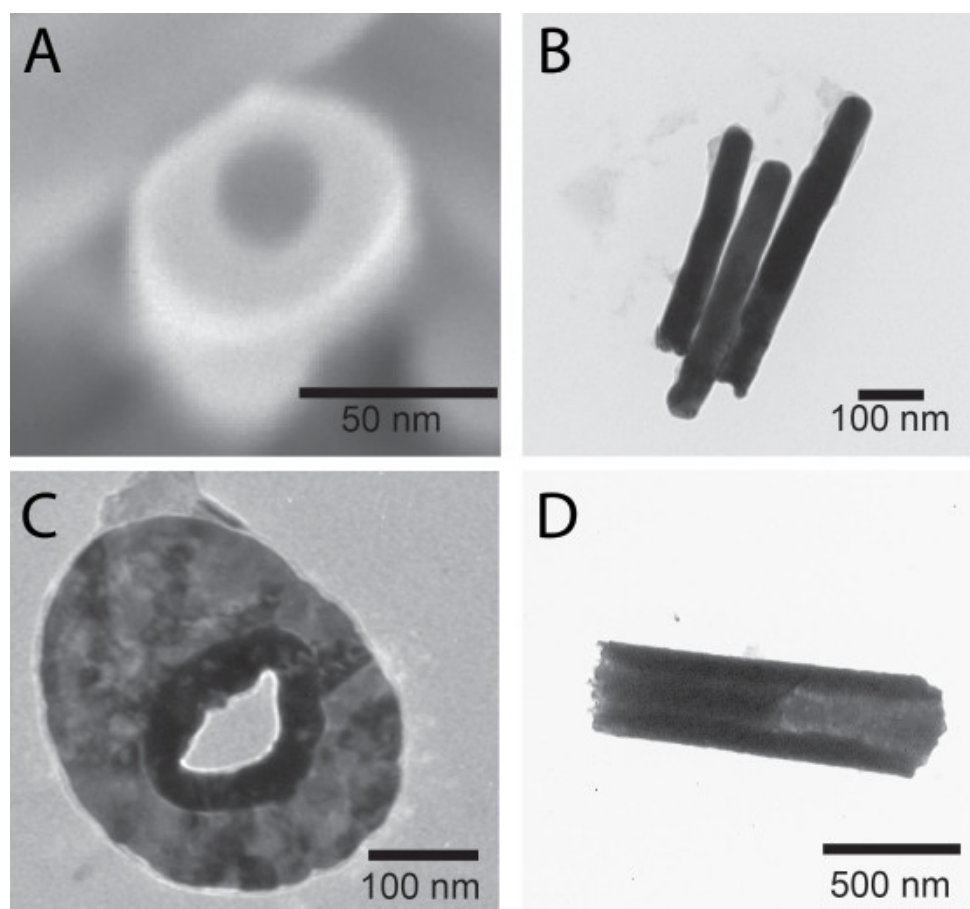


Figure 6. An SEM image of an aligned array of gold nanotubes grown off a gold substrate prepared in a 55 nm pore template (A). A TEM image of gold nanotubes prepared in a 55 nm pore template (B). A TEM cross section of a gold nanotube prepared in a 200 nm pore template (C). A TEM image of a gold nanotube prepared in a 200 nm pore template (D). Red arrows highlight the lighter contrast area of the nanotube, indicating its cavity size.

Discussion

Template directed synthesis of nanorods in AAO membranes has become increasingly popular, however syntheses of nanorods tend to be very sensitive towards minor changes in material and synthesis conditions. Here, a comprehensive understanding of the advantages and limitations of using AAO membranes is outlined, as well as a general guideline for using AAO membranes for electrochemical synthesis of nanostructures.

When purchasing AAO membranes, there are two general types available: asymmetric and symmetric. Asymmetric membranes have pore diameters that vary from the top to the bottom. The bottom of the templates typically consists of a branched network of pores, which eventually leads into an aligned, parallel array. Symmetric membranes are also available, and are typically higher quality, with uniform aligned pore diameters along the entire thickness of the membrane. Membranes of this type are preferred if the goal is to create an array of nanostructures bound to a substrate.

As purchased, AAO membranes are open at each end. The purpose of the evaporated silver layer is to form a working electrode that seals one end of the membrane. This allows each pore to act as an individual electrochemical cell during the synthesis. The following step is the electrodeposition of metal, and is required in asymmetric membranes to fill in the branched area of the membrane with non-uniform pore diameters. This step is important because without it, branched and irregular nanostructures are formed. The choice of metal is not important and depends on your desired etching conditions. Copper was used because of its high conductivity, low cost, and ease of removal, however silver, nickel, and gold can also be used.

The nickel layer is important for the electropolymerization step. The goal of this step is to form a 200-500 nm nickel coating on top of the copper to form a layer for the polymer to adhere to. Only gold and nickel have suitably high work functions to support oxidative polymerization. Gold however, cannot be etched separately from the nanotube (also composed of gold), thus using gold would result in tubes that are sealed at one end. Nickel is the only metal that can be used in this step if you require solution suspendable gold nanotubes that are open on both ends.

The polymer acts as a sacrificial core for the gold nanotube shell, however the choice of polymer and its nanotube morphology are very important. The polymer must be hydrophobic, such that it collapses onto itself upon addition of the aqueous gold plating solution rather than adhere to the template wall. This hydrophobic collapse provides a space for the gold nanotube to be deposited between the polymer core and template walls and hydrophilic polymers subjected to the same synthesis conditions do not allow for full gold tubes to form. The polymer must

also form a tube rather than a rod, as polymer rod cores (hydrophobic or hydrophilic) cannot collapse, thus not allow for gold nanotube shell deposition. The morphology of the polymer core is also affected by the solvent/electrolyte used for electropolymerization, which also affects the wall thickness of the resulting gold nanotube. A more detailed description of the mechanism of core collapse and how to control wall thickness of the resulting gold nanotubes has been recently described in literature¹⁶. In this study, we chose 3-hexylthiophene as the monomer and 46% boron trifluoride in diethyl ether as our solvent/electrolyte since it is known to produce thin walled, highly hydrophobic poly-3-hexylthiophene nanotubes^{7, 10}.

The final step is electrodepositing the gold shell. At this point it is crucial to ensure the pores of the membrane are not clogged, which prevents electrodeposition. This can be accomplished by thorough, gentle rinsing after each step, and by allowing the gold plating solution several minutes to permeate the membrane entirely before applying a potential. The easiest indication that a membrane has become clogged is a low current (below 1 μ amp/sec for the diameter of membranes described here, 13 mm). The length of the gold nanotube can be varied by increasing the deposition time.

After acid etching the base metals and polymer core, the gold nanotubes are left in the membrane. At this point their optical properties can be studied as an array, or the template can be dissolved and their homogeneous solution optical properties can be observed. When conducting optical measurements it is important to ensure all traces of water are removed and replaced with deuterium oxide, as water will interfere with the near-IR portion of the spectra where the longitudinal plasmon mode occurs. Another important consideration for optical measurements is the aggregation of gold nanotubes in solution. Unmodified gold nanotubes will aggregate if left in solution, thus brief sonication fully reverses aggregation of these nanotubes, and is required to freely suspend them prior to extinction measurements. Solutions of these gold nanotubes remain stable over periods of minutes to hours, depending on their size, before requiring further sonication.

In summary, solution-suspendable gold nanotubes can be prepared in AAO membranes. AAO membranes are useful for synthesizing arrays of high aspect ratio nanorods, and have advantages over solution based syntheses in that it is very easy to control nanoparticle dimensions. While solution based syntheses can yield more material, synthesizing complex composite or hollow nanoparticles is much more controlled using AAO membranes, and allows for the synthesis of ordered arrays.

Acknowledgements

This work was supported by the University of Toronto, the Natural Sciences and Engineering Research Council of Canada, the Canadian Foundation for Innovation, and the Ontario Research Fund. DSS thanks the Ontario Ministry for an Early Researcher Award.

References

1. Lee, W., Ji, R., Gösele, U., & Nielsch, K. Fast fabrication of long-range ordered porous alumina membranes by hard anodization. *Nature Publishing Group*. **5**, (9) 741-747 (2006).
2. Li, F., Zhang, L., & Metzger, R.M. On the growth of highly ordered pores in anodized aluminum oxide. *Chemistry of Materials*. **10**, (9) 2470-2480 (1998).
3. Martin, C.R. Template synthesis of electronically conductive polymer nanostructures. *Accounts of Chemical Research*. **28**, (2) 61-68 (1995).
4. Martin, C.R. Membrane-based synthesis of nanomaterials. *Chemistry of Materials*. **8**, (8) 1739-1746 (1996).
5. Possin, G.E. A method for forming very small diameter wires. *Review of Scientific Instruments*. **41**, (5) 772-774 (1970).
6. Goad, D.G.W. & Moskovits, M. Colloidal metal in aluminum-oxide. *Journal of Applied Physics*. **49**, (5) 2929-2934 (1978).
7. Huesmann, D., DiCarmine, P.M., & Seferos, D.S. Template-synthesized nanostructure morphology influenced by building block structure. *Journal of Materials Chemistry*. **21**, (2) 408 (2011).
8. Steinhart, M., Wendorff, J.H., et al. Polymer nanotubes by wetting of ordered porous templates. *Science*. **296**, (5575) 1997 (2002).
9. Hulteen, J.C. & Martin, C.R. A general template-based method for the preparation of nanomaterials. *Journal of Materials Chemistry*. **7**, (7) 1075-1087 (1997).
10. DiCarmine, P.M., Fokina, A., & Seferos, D.S. Solvent/Electrolyte Control of the Wall Thickness of Template-Synthesized Nanostructures. *Chemistry of Materials*. **23**, (16) 3787-3794 (2011).
11. Wei, W., Li, S., et al. Surprisingly long-range surface-enhanced Raman scattering (SERS) on Au-Ni multisegmented nanowires. *Angewandte Chemie International Edition*. **48**, (23) 4210-4212 (2009).
12. Qin, L., Zou, S., Xue, C., Atkinson, A., Schatz, G.C., & Mirkin, C.A. Designing, fabricating, and imaging Raman hot spots. *Proceedings of the National Academy of Sciences of the United States of America*. **103**, (36) 13300-13303 (2006).
13. Ruan, C., Eres, G., Wang, W., Zhang, Z., & Gu, B. Controlled Fabrication of Nanopillar Arrays as Active Substrates for Surface-Enhanced Raman Spectroscopy. *Langmuir*. **23**, (10) 5757-5760 (2007).
14. McPhillips, J., Murphy, A., et al. High-Performance Biosensing Using Arrays of Plasmonic Nanotubes. *ACS Nano*. **4**, (4) 2210-2216 (2010).
15. Bridges, C.R., DiCarmine, P.M., & Seferos, D.S. Gold Nanotubes as Sensitive, Solution-Suspendable Refractive Index Reporters. *Chemistry of Materials*. **24**, (6) 963-965 (2012).
16. Bridges, C.R., DiCarmine, P.M., Fokina, A., Huesmann, D., & Seferos, D.S. Synthesis of Gold Nanotubes with Variable Wall Thicknesses. *Journal of Materials Chemistry A*. **1**, 1127-1133 (2013).
17. Kennedy, L.C., Bickford, L.R., et al. A New Era for Cancer Treatment: Gold-Nanoparticle-Mediated Thermal Therapies. *Small*. **7**, (2) 169-183 (2010).
18. Lee, S.B. & Martin, C.R. pH-Switchable, Ion-Permeable Gold Nanotubule Membrane Based on Chemisorbed Cysteine. *Analytical Chemistry*. **73**, (4) 768-775 (2001).
19. Velleman, L., Shapter, J.G., & Losic, D. Gold nanotube membranes functionalised with fluorinated thiols for selective molecular transport. *Journal of Membrane Science*. **328**, (1-2) 121-126 (2009).
20. Sanchez-Castillo, M.A., Couto, C., Kim, W.B., & Dumesic, J.A. Gold-Nanotube Membranes for the Oxidation of CO at Gas-Water Interfaces. *Angewandte Chemie (International ed. in English)*. **43**, (9) 1140-1142 (2004).

21. Kim, B.Y., Swearingen, C.B., Ho, J.-A.A., Romanova, E.V., Bohn, P.W., & Sweedler, J.V. Direct Immobilization of Fab' in Nanocapillaries for Manipulating Mass-Limited Samples. *Journal of the American Chemical Society*. **129**, (24) 7620-7626 (2007).
22. Delvaux, M., Walcarius, A., & Demoustier-Champagne, S. Electrocatalytic H₂O₂ amperometric detection using gold nanotube electrode ensembles. *Analytica Chimica Acta*. **525**, (2) 221-230 (2004).
23. Kohli, P., Wirtz, M., & Martin, C.R. Nanotube Membrane Based Biosensors. *Electroanalysis*. **16**, (12) 9-18 (2004).
24. Ruppini, R. *Electromagnetic Surface Modes*. John Wiley & Sons: New York, (1982).
25. Sonnichsen, C. *Plasmons in Metal Nanostructures*. Culliver Verlag: Gottingen, (2001).
26. Barnes, W.L., Dereux, A., & Ebbesen, T.W. Surface plasmon subwavelength optics. *Nature*. **424**, 824-830 (2003).
27. Maier, S.A., Kik, P.G., *et al.* Local detection of electromagnetic energy transport below the diffraction limit in metal nanoparticle plasmon waveguides. *Nature Materials*. **2**, (4) 229-232 (2003).
28. Barhoumi, A., Zhang, D., Tam, F., & Halas, N.J. Surface-Enhanced Raman Spectroscopy of DNA. *Journal of the American Chemical Society*. **130**, (16) 5523-5529 (2008).
29. Yin, J., Wu, T., *et al.* SERS-Active Nanoparticles for Sensitive and Selective Detection of Cadmium Ion (Cd²⁺). *Chemistry of Materials*. **23**, (21) 4756-4764 (2011).
30. Schmucker, A.L., Harris, N., *et al.* Correlating Nanorod Structure with Experimentally Measured and Theoretically Predicted Surface Plasmon Resonance. *ACS Nano*. **4**, (9) 5453-5463 (2010).
31. Payne, E.K., Shuford, K.L., Park, S., Schatz, G.C., & Mirkin, C.A. Multipole Plasmon Resonances in Gold Nanorods. *The Journal of Physical Chemistry B*. **110**, (5) 2150-2154 (2006).
32. Moskovits, M. Surface-enhanced spectroscopy. *Reviews of Modern Physics*. **57**, (3) 783 (1985).
33. Sieb, N.R., Wu, N.-C., Majidi, E., Kukreja, R., Branda, N.R., & Gates, B.D. Hollow metal nanorods with tunable dimensions, porosity, and photonic properties. *ACS Nano*. **3**, (6) 1365-1372 (2009).
34. Muench, F., Kunz, U., Neetzel, C., Lauterbach, S., Kleebe, H.-J., & Ensinger, W. 4-(Dimethylamino)pyridine as a Powerful Auxiliary Reagent in the Electroless Synthesis of Gold Nanotubes. *Langmuir*. **27**, (1) 430-435 (2011).
35. Wirtz, M. & Martin, C.R. Template-Fabricated Gold Nanowires and Nanotubes. *Advanced Materials*. **15**, (5) 455-458 (2003).
36. Sehayek, T., Lahav, M., Popovitz-Biro, R., Vaskevich, A., & Rubinstein, I. Template Synthesis of Nanotubes by Room-Temperature Coalescence of Metal Nanoparticles. *Chemistry of Materials*. **17**, (14) 3743-3748 (2005).
37. Lahav, M., Sehayek, T., Vaskevich, A., & Rubinstein, I. Nanoparticle Nanotubes. *Angewandte Chemie (International ed. in English)*. **42**, (45) 5576-5579 (2003).
38. Hua, Z., Yang, S., *et al.* Metal nanotubes prepared by a sol-gel method followed by a hydrogen reduction procedure. *Nanotechnology*. **17**, (20) 5106-5110 (2006).
39. Lee, W., Scholz, R., Nielsch, K., & Gösele, U. A Template-Based Electrochemical Method for the Synthesis of Multisegmented Metallic Nanotubes. *Angewandte Chemie (International ed. in English)*. **44**, (37) 6050-6054 (2005).
40. Cui, C.-H., Li, H.-H., & Yu, S.-H. A general approach to electrochemical deposition of high quality free-standing noble metal (Pd, Pt, Au, Ag) sub-micron tubes composed of nanoparticles in polar aprotic solvent. *Chemical Communications*. **46**, (6) 940 (2010).
41. Han, X.-F., Shamaila, S., Sharif, R., Chen, J.-Y., Liu, H.-R., & Liu, D.-P. Structural and Magnetic Properties of Various Ferromagnetic Nanotubes. *Advanced Materials*. **21**, (45) 4619-4624 (2009).
42. Hendren, W.R., Murphy, A., *et al.* Fabrication and optical properties of gold nanotube arrays. *Journal of Physics: Condensed Matter*. **20**, (36) 362203 (2008).
43. Lahav, M., Weiss, E.A., Xu, Q., & Whitesides, G.M. Core-Shell and Segmented Polymer-Metal Composite Nanostructures. *Nano Letters*. **6**, (9) 2166-2171 (2006).
44. Chen, X., Li, S., Xue, C., Banholzer, M.J., Schatz, G.C., & Mirkin, C.A. Plasmonic Focusing in Rod-Sheath Heteronanostructures. *ACS Nano*. **3**, (1) 87-92 (2009).
45. Banholzer, M.J., Qin, L., Millstone, J.E., Osberg, K.D., & Mirkin, C.A. On-wire lithography: synthesis, encoding and biological applications. *Nature Protocols*. **4**, (6) 838-848 (2009).